

Received September 21, 2021, accepted October 22, 2021, date of publication October 27, 2021, date of current version November 18, 2021.

Digital Object Identifier 10.1109/ACCESS.2021.3123727

Application Research of Fuzzy PID Control Optimized by Genetic Algorithm in Medium and Low Speed Maglev Train Charger

LI ZHANG¹, LIWEI ZHANG¹, JIAWEI YANG², MING GAO¹, AND YINGHUA LI¹

¹CRRC Tangshan Company, Ltd., Tangshan 064000, China

²College of Electrical Engineering, Ministry of Education, Beijing Jiaotong University, Beijing 100044, China

Corresponding author: Liwei Zhang (lwzhang@bjtu.edu.cn)

ABSTRACT China's railways are developing rapidly, and the charger of the auxiliary power supply system is an indispensable part of the maglev train. The existing maglev train charger usually uses the traditional PID controller to control the output of the charger which has a simple structure. To meet the requirements of the maglev train charger output performance which is getting higher and higher, it is necessary to optimize the control strategies which can achieve adaptive control of the system. In this paper, taking Qingyuan maglev train as the research object, the control principle of the charger of the maglev train is studied, and the simulation model of the charger of Qingyuan speed maglev train is built in MATLAB/Simulink. After verifying its feasibility, the paper proposes fuzzy PID control to improve the charger control method, and uses genetic algorithm to optimize fuzzy control membership function and fuzzy rules. Finally, the paper builds a fuzzy PID controller simulation model, compares the output performance of the charger under different control methods, and verifies the superiority of the new control method.

INDEX TERMS Maglev train, charger, fuzzy PID, genetic algorithm.


I. INTRODUCTION

Qingyuan maglev train has the advantages of small turning radius, low energy consumption and comfort, which has great potential in the development of urban transportation. The auxiliary power supply system of medium and low speed maglev train is one of the important components of the maglev train electrical system mainly composed of auxiliary converter, charger, suspension power supply, battery pack and load [1]–[3]. The main function of the auxiliary power supply system is to provide the electric energy of the maglev train in addition to the traction motor. Among them, the charger plays an important role of the whole train, which charges the emergency battery and powers the DC load including the train lighting facility, the DC cooling fan, the DC water heater, and the train control system.

Maglev train charger technology mainly realizes the control of battery charging and DC load power supply by combining power electronics, signal processing and automatic control principles [4], [5]. Among them, the reference [6] proposed a fast charging strategy, and the

constantly updated charging strategy has higher requirements for the output accuracy of the charger.

The actual charger usually uses conventional PID control for closed-loop control to ensure the reliability of battery charging and the safety of DC load operation [7]. At present, there is little literature to analyze the control method of the charger for maglev train. Literature [4], [8], [9] mainly studies the topology and control of auxiliary converter of maglev train, Literature [10] designs and studies the magnetic suspension power system. Literature [11] proposes the control optimization of the integrated power system. Literature [12] studies the control method of the independent photovoltaic charging module of lead-acid battery. Literature [13] simulates the electric vehicle charging module and studies the influence of the optimized control method on the output of the charger. Little research has been put on the optimization of charger control method in maglev trains, therefore, the paper expect to study the charger topology and control method of the Qingyuan maglev train, and introduce fuzzy control technology to optimize the charger control method of maglev train, in order to solve the problem of weak anti-interference of conventional PID in the working process of charger, and optimize the fuzzy PID control

The associate editor coordinating the review of this manuscript and approving it for publication was Mohsin Jamil .

method by genetic algorithm to further improve the output effect of charger. When studying the fuzzy PID control, it is found that the parameters of the fuzzy control membership function are difficult to determine, and the fuzzy rules are not completely consistent with the charging control system. In order to further improve the output performance of the charger, based on the fuzzy PID control, the genetic algorithm is used to encode and optimize the membership function and fuzzy control rules in the fuzzy control. Thus, the optimal membership function distribution and the optimal fuzzy control rules of the charger are determined. It has certain research significance for the follow-up research of charger optimization of the Qingyuan maglev train in China.

In this paper, genetic algorithm is proposed to encode and optimize the membership function and control rules of fuzzy PID, ITAE Criterion is selected as the optimization standard, new membership function graphics and control rules are obtained, and the optimization process is realized by programming in MATLAB. This paper compares the charger output characteristics of different control methods in three cases, and determines the optimization effect of genetic algorithm on Fuzzy PID membership function and fuzzy control rules. The optimized fuzzy PID control charger has good output performance and small output charging current fluctuation, Finally, the simulation verifies whether the charger under the new control method can basically meet the output accuracy requirements of the optimized segmentation strategy. The paper selects Qingyuan maglev train as the research object to study the control method of its charger, the maglev train charger model is built, and after verifying the feasibility of the model, the paper proposes fuzzy PID control method, uses genetic algorithm to optimize the membership and control rules of the fuzzy PID control. The paper compares the output results of the charger under different control methods, and analyzes the advantages of the genetic algorithm to optimize the fuzzy PID control method.

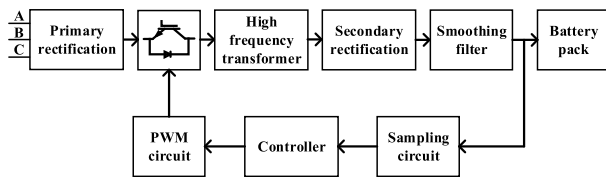


FIGURE 1. Overall schematic diagram of charger.

II. RESEARCH ON QINGYUAN MAGLEV TRAIN
A. QINGYUAN MAGLEV TRAIN CHARGER TOPOLOGY

Qingyuan maglev train is a new generation of medium and low speed maglev train independently developed by CSR Tangshan company. Figure 1 shows the block diagram of the auxiliary power supply system charger of the Qingyuan medium and low speed maglev train. The charger converts the three-phase 380V AC power output from the front-end auxiliary converter into DC power through the rectification and filtering process, and then provides power to DC loads

such as the battery pack after inverter, transformer, filter, secondary rectification, and smooth filtering [4], [8], [9].

The main components of the charger for the auxiliary power supply system of Qingyuan maglev train include a three-phase uncontrolled bridge rectifier circuit and a DC bridge converter circuit. The topology of the charger is shown in Figure 2.

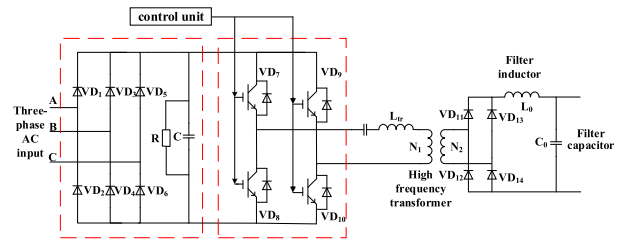


FIGURE 2. Topology of charger in auxiliary power supply system of Qingyuan maglev train.

B. ANALYSIS OF CLOSED-LOOP CONTROL
MODEL OF CHARGER

The charger is composed of an uncontrolled bridge rectifier circuit and a DC full-bridge converter. The uncontrolled rectifier bridge circuit does not require a control unit. Therefore, the closed-loop control system of the charger is a full-bridge switching converter model, and the topology of the full-bridge converter is shown in Figure 3.

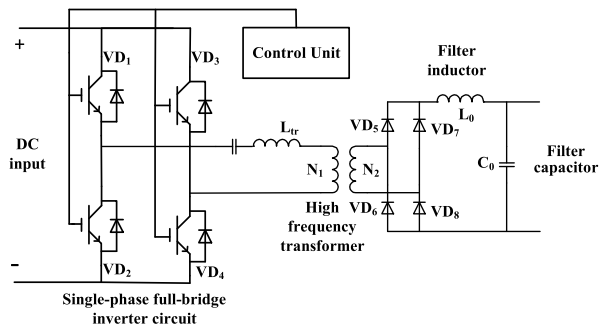


FIGURE 3. Circuit of full bridge converter.

The full-bridge converter model is a time-varying system and the calculation process is complicated. Therefore, it is necessary to simply the model. The simplified circuit of the full-bridge converter is shown in Figure 4:

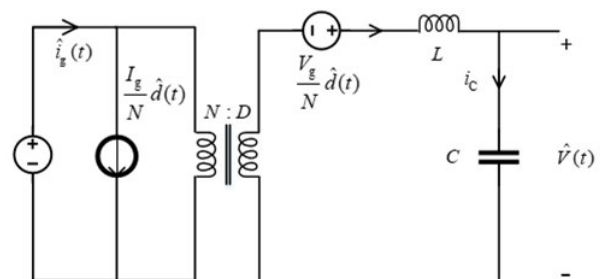


FIGURE 4. AC linear model equivalent circuit of full bridge converter.

The mathematical formula of the simplified model of the full-bridge converter with transformer is as follows:

$$\begin{cases} L \frac{d\hat{i}_L(t)}{dt} = \frac{V_g \hat{d}(t)}{N} + \frac{D}{N} \hat{v}_g(t) - \hat{v}(t) \\ C \frac{d\hat{v}(t)}{dt} = \hat{i}_L(t) = \frac{\hat{v}(t)}{R} \\ \hat{i}_g(t) = \frac{D\hat{i}_L(t)}{N} + \frac{I_L}{N} \hat{d}(t) \end{cases} \quad (1)$$

I_L, V_g, D are the inductor current, input voltage, duty cycle, $\hat{i}_L(t), \hat{v}_g(t), \hat{d}(t), \hat{v}(t)$ are small signal fluctuations of inductor current, input voltage, duty cycle and output voltage.

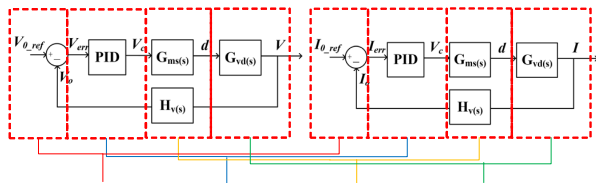


FIGURE 5. Constant-voltage closed-loop control and constant-current closed-loop control block diagram.

The control strategy commonly used in charger simulation is the output single-closed-loop feedback control strategy. Figure 5 shows the control block diagram when the charger works under constant-voltage closed-loop control or constant-current closed-loop control. The two both calculate the error signal according to the feedback amount and the expected value. The control amount V_c is calculated by the PID transfer function and generates a duty cycle signal d through bipolar PWM modulation method. The duty cycle signal d controls the charger switching full-bridge converter to complete closed-loop control.

The charger outputs a specific value according to the state of charge of the battery pack. Because the charging method of the battery pack needs to be controlled in different charging stages, the voltage PID closed-loop control strategy and the current PID closed-loop control strategy are combined to control the charger output. The charger control block diagram is shown in Figure 6.

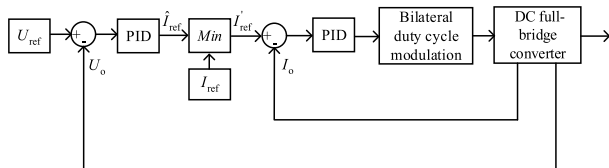


FIGURE 6. Double closed-loop control block diagram of charger.

C. SIMULATION ANALYSIS OF POWER SUPPLY SYSTEM FOR QINGYUAN MAGLEV TRAIN

Based on MATLAB®/Simulink® platform, the simulation model of Qingyuan maglev train charger is built and the parameters of the auxiliary charger of Qingyuan maglev train are shown in Table 1.

In order to simplify the simulation, the paper chooses the ideal three-phase AC power supply to provide AC voltage

TABLE 1. Charger simulation parameters.

parameter	value
Charger input	AC380V/50Hz
Charger filter inductance / capacitor	50μH/6000μF
Transformer ratio	3: 1
Switch sampling frequency f_s	15 kHz
charger rated power P_2	16 kW
Charger voltage output $u_{0-charger}$	DC110V (77-126V)

for the charger, and the charger supplies power for the later-stage load after starting. Figure 7 shows the overall simulation model of the charging system of Qingyuan maglev train.

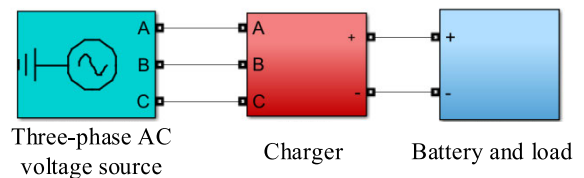


FIGURE 7. Simulation model of charger of Qingyuan maglev train.

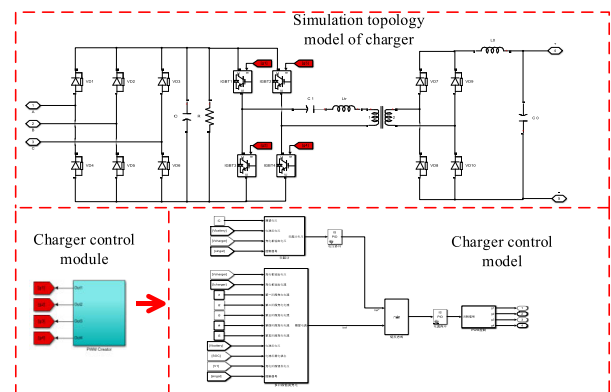


FIGURE 8. Charger simulation model of Qingyuan maglev train.

Figure 8 shows the simulation model of charger for Qingyuan maglev train.

Through simulation, the start-up waveform of the charger is shown in figure 9 and the output waveform under the DC load switching mode of the charger is shown in figure 10. The expected voltage set is 115V.

It can be seen from the above waveforms that the charger output voltage responds faster to DC115V, and output fluctuation is less than 5%. There is no significant change in voltage when switching the load, which meets the actual system parameter requirements.

Figure 11 and Figure 12 show the experimental platform of auxiliary converter and charger for Qingyuan maglev train respectively. Figures 13 and 14 are the charger voltage and current output waveforms of the experimental platform when the charger is started and when the charger is put into the load respectively.

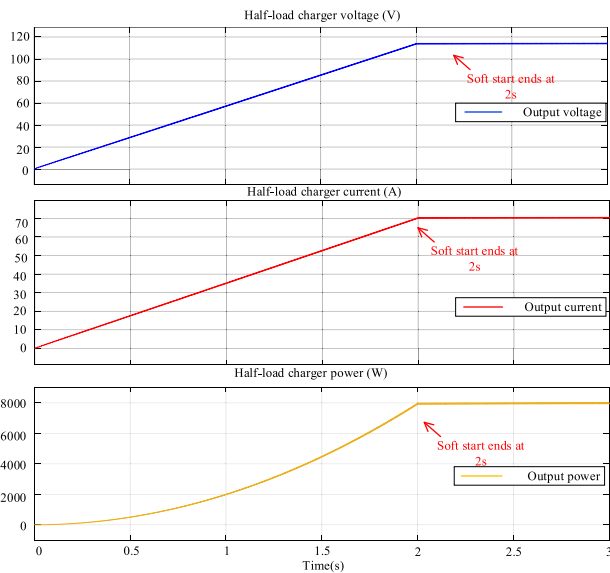


FIGURE 9. Charger start simulation waveform.

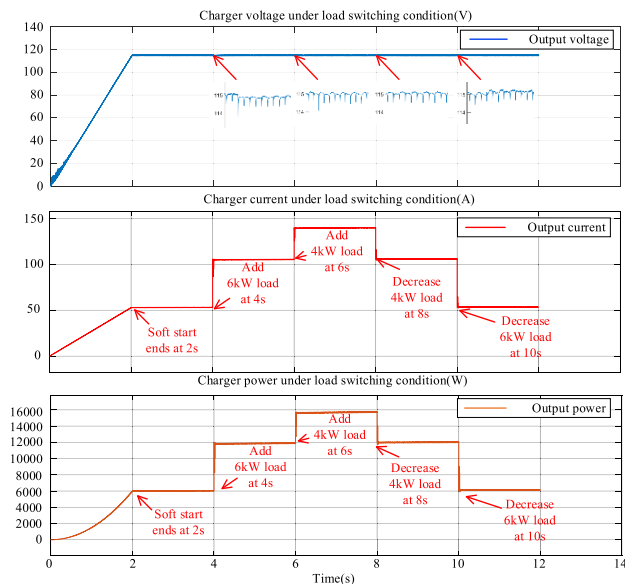


FIGURE 10. Charger simulation waveform under load switching condition.

Comparing the experimental results, it can be seen that the output voltage and output current of the simulation model are consistent with the change trend of the platform experimental results during the operation process, so the simulation model can be subjected to subsequent experiments.

III. FUZZY PID CONTROL SYSTEM BASED ON GENETIC ALGORITHM OPTIMIZATION

A. FUZZY PID CONTROL METHOD

The traditional PID control cannot realize the adaptive tuning of PID parameters. In order to further improve the output performance of the charger, the fuzzy PID control algorithm is used to adjust the charger system.

The basic idea of fuzzy PID control is to transform the actual measured exact value into a fuzzy quantity, establish



FIGURE 11. Experimental platform for auxiliary converter of Qingyuan maglev train.



FIGURE 12. Qingyuan maglev train charger experimental platform.

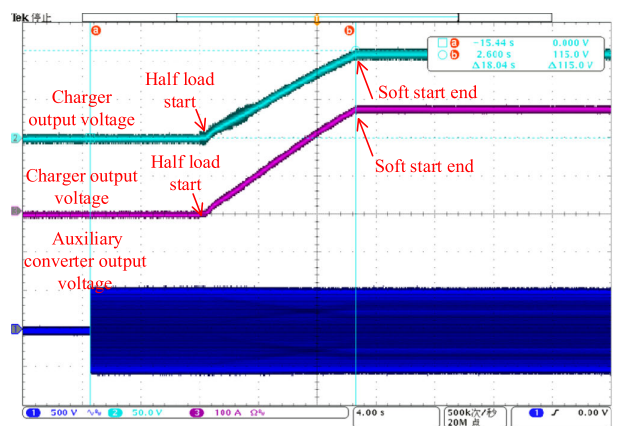


FIGURE 13. Output waveform when the charger starts.

a fuzzy inference rule base according to the set fuzzy rules, get the specific control quantity after fuzzy reasoning and

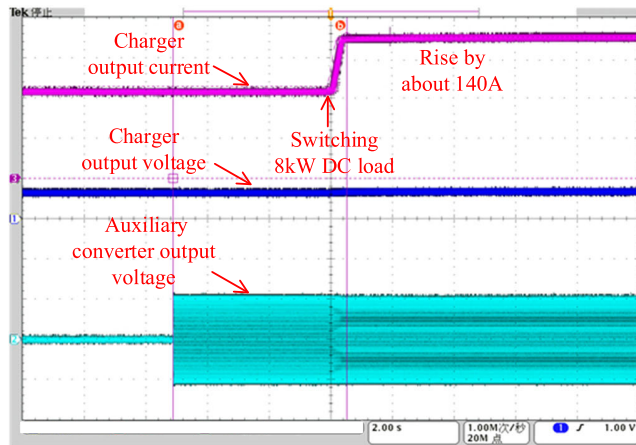


FIGURE 14. Charger output waveform under load switching conditions.

de-fuzzy, and complete the control flow [10]–[13]. In this paper, the shape of the fuzzy membership function selects the triangle, and the deblurring method selects center-of-gravity defuzzification.

In this paper, e and ec are taken as the input of the fuzzy control, e is the deviation between the expected output and the actual output and ec is the rate of e . The PID parameter correction ΔK_p , ΔK_i and ΔK_d are selected as output. The transformation between the fuzzy quantity and the determined value is realized through the scale factor and the function $f(K_e, e), f(K_{ec}, ec), f(K_{\Delta kp}, \Delta kp), f(K_{\Delta ki}, \Delta ki), f(K_{\Delta kd}, \Delta kd)$, and the process is shown in figure 15.

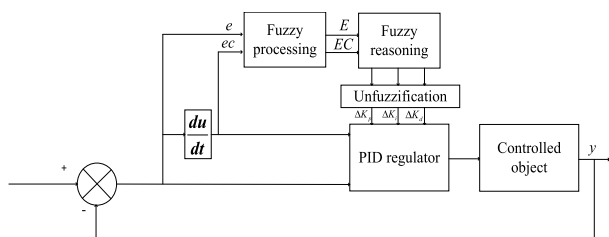


FIGURE 15. Fuzzy adaptive PID flow chart.

The fuzzy domain of the fuzzy controller is divided into seven cases {negative big, negative medium, negative small, zero, positive small, median, positive big}, expressed by the letters {NB, NM, NS, ZO, PS, PM, PB}. According to the range of the fuzzy controller input e' and ec' in the fuzzy domain after the transformation of the scale factor, the input parameters can be blurred into language values to realize fuzzification. The fuzzy rules are shown in Table 2.

Considering that the expected output of the charger in different stages of the charger charging strategy is different, and the variation range of the input e of the fuzzy controller is different, the calculation formula of the scale factor of the input e of the corresponding fuzzy controller is shown in (2):

$$K_{ek} = \frac{E_k}{\gamma_k L_k}, \quad k = 1, 2, 3, \dots \quad (2)$$

k is the number of stages of the charging strategy of the charger; K_{ek} is the corresponding scale factor; L_k is the

TABLE 2. Fuzzy PID control rules.

$\Delta K_p, \Delta K_i,$		ec						
		NB	NM	NS	ZO	PS	PM	PB
e	NB	PB/N B/PS	PB /NB/ NS	PM/ NM/ NB	PM/ NM/ NB	PS/N S/N B	ZO/Z O/N M	ZO/Z O/PS
	N	PB/N B/PS	PB/N B/NS	PM/ NM/ NB	PS/N S/N M	PS/N S/N M	ZO/Z O/N S	NS/Z O/Z O
	NS	PM/ NB/ ZO	PM/ NM/ NS	PM/ NS/N S	PS/N S/N M	ZO/ ZO/ NS	NS/P S/NS	NS/P S/ZO
	ZO	PM/ NM/ ZO	PM/ NM/ NS	PS/N S/NS	ZO/Z O/NS	NS/P S/NS	NM/ PM/ NS	NM/ PM/ ZO
	PS	PS/N S/ZO	PS/N S/ZO	ZO/Z O	NS/P S/ZO	NS/P S/ZO	NM/ PM/ ZO	NM/ PM/ ZO
	PM	PS/Z O/PB	ZO/Z O/N S	NS/P S/PS	NM/ PM/P S	NM/ PM/ PS	NM/ PB/P S	NB/P B/PB
	PB	ZO/Z O/PB	ZO/Z O/P M	NM/ PS/P M	NM/ PM/P M	NM/ PB/P S	NB/P B/PS	NB/P B/PB

maximum value of the input e of the fuzzy controller at the corresponding stage; E_k is the boundary value of the input fuzzy universe. The paper introduces the input scale factor calculation coefficient γ_k to adjust the value of the scale factor.

The calculation formula of the scale factor corresponding to the input ec of the fuzzy controller is shown in formula (3):

$$K_{ec} = \frac{EC}{\sigma ec_{max}} \quad (3)$$

K_{ec} is the scale factor corresponding to the input ec of the fuzzy controller, EC is the boundary value of the input fuzzy domain, ec_{max} is the maximum value of the input ec of the fuzzy controller, the scale factor calculation coefficient σ is usually in the range of 0.3-0.9.

$K_{\Delta kp}, K_{\Delta ki}, K_{\Delta kd}$ are the scale factors of the fuzzy controller outputs $\Delta K_p, \Delta K_i, \Delta K_d$. The calculation formula is as follows:

$$\begin{cases} K_{\Delta kp} = \frac{\omega_{kp} k_{pmax}}{Y_{kp}} \\ K_{\Delta ki} = \frac{\omega_{ki} k_{imax}}{Y_{ki}} \\ K_{\Delta kd} = \frac{\omega_{kd} k_{dmax}}{Y_{kd}} \end{cases} \quad (4)$$

Y_{kp}, Y_{ki}, Y_{kd} are the maximum values of the corresponding output fuzzy domain, $k_{pmax}, k_{imax}, k_{dmax}$ are the parameters of the closed-loop PID, respectively. $\omega_{kp}, \omega_{ki}, \omega_{kd}$ are the calculation coefficients of the scale factor of the output of the fuzzy controller.

B. FUZZY PID CONTROL OPTIMIZED BY GENETIC ALGORITHM

The membership function parameters of fuzzy PID control are usually determined by experience, which is lack of

objectivity, and the fuzzy rules do not necessarily match with the charger. Therefore, this paper uses genetic algorithm to optimize fuzzy PID control parameters to improve the control effect [14].

Genetic algorithm is a kind of optimization algorithm developed by simulating the rule of “survival of the fittest” in the real nature. Its essence is to simulate the way in which natural biological chromosome genes cross and mutate to form new individuals, and to generate the optimal solution by iteration. The basic steps include coding, establishing objective function, selection, crossover and mutation. The genetic algorithm optimization process is shown in figure 16.

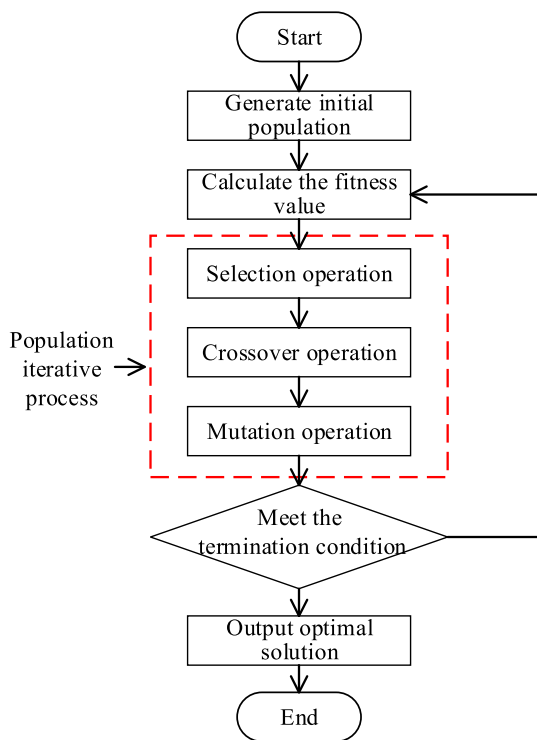


FIGURE 16. Optimization process of genetic algorithm.

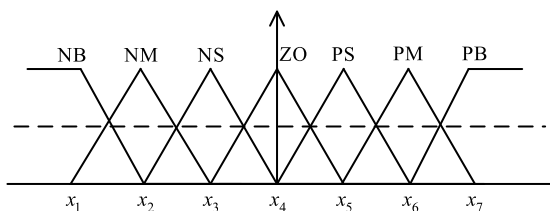


FIGURE 17. Optimization process of genetic algorithm.

The paper expects to optimize the membership function and fuzzy rules of fuzzy control. First of all, the fuzzy membership function is encoded in the form of floating point number, and the endpoint $\{x_1, x_2, x_3, \dots, x_7\}$ at the bottom of the triangle membership function is selected as the optimization parameter, as shown in figure 17. For the fuzzy inference system with two inputs and three outputs, the membership function coding is composed of input codes $\{x_1^e, x_2^e, x_3^e, \dots, x_7^e\}$, $\{x_1^{ec}, x_2^{ec}, x_3^{ec}, \dots, x_7^{ec}\}$, output codes $\{x_1^{kp}, x_2^{kp}, x_3^{kp}, \dots, x_7^{kp}\}$,

TABLE 3. Fuzzy PID control rules.

$\Delta K_p, \Delta K_i,$	e_c						
	001	010	011	100	101	110	111
00	111/0	111/0	110/0	110/0	101/	100/	100/
1	01/1	01/0	01/0	10/0	010/	100/	100/
	01	11	01	01	001	010	101
01	111/0	111/0	110/0	101/	101/	100/	011/1
0	01/1	01/0	10/0	010/	011/0	100/	00/1
	01	11	01	010	10	011	00
01	110/	110/	110/0	101/	100/	011/1	011/1
1	010/	010/	11/01	011/0	100/	01/01	01/1
	100	011	0	10	011	1	00
10	110/	110/	101/	100/	011/1	010/	010/1
e_c	0	010/	011/	011/0	100/	01/01	101/
	100	011	11	011	1	011	00
10	101/	101/	100/	011/1	011/1	010/1	010/1
1	011/	011/	100/	01/1	01/1	10/1	10/1
	100	100	100	00	00	00	00
11	101/	100/	011/1	010/1	010/1	010/1	001/1
0	011/1	100/	01/1	10/1	10/1	11/10	11/11
	11	011	01	01	01	1	1
11	100/	100/	010/	010/1	010/1	001/1	001/1
1	100/	100/	101/1	10/11	10/1	11/10	11/11
	111	110	10	0	01	1	1

$\{x_1^{ki}, x_2^{ki}, x_3^{ki}, \dots, x_7^{ki}\}$ and $\{x_1^{kd}, x_2^{kd}, x_3^{kd}, \dots, x_7^{kd}\}$. When the genetic algorithm is running, the variation range of $\{x_1, x_2, x_3, \dots, x_7\}$ needs to be set.

Secondly, the control rules are encoded by binary code string, and the seven language values of fuzzy language variables are represented by 3-bit binary numbers to realize the digital coding of fuzzy control table. Table 3 shows the digital fuzzy control table.

Based on the above compilation of control rules, the coding of 3×49 -bit control rules is obtained, and then the optimal value of control rules is obtained by genetic algorithm optimization.

The genetic algorithm takes the fitness function as the result of the optimization process to observe the optimization effect, and uses the fitness function of the expressions (5) and (6) to evaluate the performance of the controller.

$$J = \int_0^t \tau |Y(\tau) - y_{out}(\tau)| d\tau \quad (5)$$

$$F = \frac{1}{J + 1} \quad (6)$$

In the expression, t_n is the working duration of the controller, Y is the expected output given by the system, and y_{out} is the actual output response of the system. The smaller the value of J is, the better the performance of the control system is.

The selection operation is the operation method used by the genetic algorithm to select the genetic matrix. In this paper, the roulette method is used to equate the optimization results of different fitness to the regions with different areas in the roulette. The chromosome is selected as the genetic matrix through the position of the random function on the roulette.

Crossover operation is a method to simulate the genetic exchange of genes on actual chromosomes. In this paper,

single-point crossover is used to complete the genetic maternal gene exchange according to the crossover probability.

The mutation operation simulates the chromosome variation in the iterative process of the actual population according to the mutation probability to avoid the local convergence of the optimization.

The parameters that need to be set in the execution process include: population level M , population chromosome cross transfer probability P_c , gene mutation probability P_m , genetic algebra T , when M and T are too small, the optimization result is not ideal, when M and T are too large, the iteration time is more. When the crossover probability P_c is large, the probability of recombination individuals is high and the convergence is fast, but at the same time, the replacement of old and new is too fast, and the phenomenon of premature elimination may occur. Therefore, this paper chooses $M = 50, P_c = 0.8, P_m = 0.01, T = 50$.

C. THE RESULT OF OPTIMIZING FUZZY PID BY GENETIC ALGORITHM

1) FUZZIFICATION OF INPUT

In order to simplify the operation, the input scale factor calculation formula is divided into two cases, where an is the expected charging current of the battery in the current charging stage.

$$K_e = \begin{cases} 0.15, & I_n \geq 24A \\ 0.25, & I_n < 24A \end{cases} \quad (7)$$

The scale factor $K_{ec} = 0.001$.

2) DEFUZZIFICATION OF OUTPUT

The paper mainly focuses on the optimization of the current loop of the double closed-loop PID control system. Through trial and error method, the values of the conventional PID parameters K_{p0}, K_{i0}, K_{d0} of the current loop are 1.5, 15, 0.02, the scope of the output domain is $[-6, 6]$. Output scale factor calculation coefficient $\omega_{kp} = 0.65, \omega_{ki} = 0.85, \omega_{kd} = 0.4$. After the output of the fuzzy controller is obtained, the actual PID parameters for control are obtained according to the following formula.

$$\begin{cases} K_p = K_{p0} + \Delta K_p \\ K_i = K_{i0} + \Delta K_i \\ K_d = K_{d0} + \Delta K_d \end{cases} \quad (8)$$

3) ESTABLISHMENT AND OPTIMIZATION OF FUZZY RULES

After genetic algorithm optimization, the triangle membership function bottom endpoint matrix of the input and output of the fuzzy controller is obtained, and the e membership function bottom endpoint matrix is $[-5.4576, -3.7893, -2.5131, -0.5089, 1.6678, 4.2759, 5.6460]$, and the ec membership function bottom endpoint matrix is $[-5.5548, -3.2749, -2.1234, 0.6155, 2.8555, 4.6359, 5.6747]$. The output membership function bottom edge endpoint matrix of K_p, K_i, K_d are $[-6.3146, -4.0020, -1.6361, -0.6782,$

$1.3340, 3.8661, 6.7715], [-6.2051, -3.0129, 1.7914, 0.0276, 2.4579, 4.2189, 6.8223], [-6.0804, -3.0269, -1.1702, 0.9326, 2.8828, 4.1159, 5.5352]$.

The optimized fuzzy rules are shown in Table 4:

TABLE 4. Fuzzy PID control rules.

$\Delta K_p, \Delta K_i,$	ec						
	NB	NM	NS	ZO	PS	PM	PB
NB	NB/	PS/P	NB/	NS/Z	NM/	NB/P	PM/P
	ZO/P	M/Z	NB/	O/P	NB/P	M/P	S/NB
	S	O	NS	M	M	M	
N	NS/	PM/P	ZO/	NB/	NM/	PS/N	ZO/P
	NM/	M/N	NB/	ZO/Z	NB/P	S/N	M/Z
M	PM	M	PM	O	S	M	O
	PM/	PM/	NS/	PM/	NM/	NB/P	NB/P
NS	PS/P	NB/	ZO/	NM/	NS/N	M/N	M/N
	S	NB	NB	ZO	S	S	B
e	ZO/	ZO/P	ZO/	NB/P	PS/Z	ZO/	PM/
	NS/P	S/PS	NS/	M/P	O/NS	NM/	NS/N
	M		ZO	M		PS	M
PS	PM/	ZO/Z	NS/	NM/	NB/	ZO/P	ZO/
	NM/	O/N	NS/	NB/	NM/	S/PM	NM/
	ZO	M	NM	NS	NS		NM
PM	PS/P	NM/	NB/	PM/	NS/N	NB/P	ZO/Z
	M/P	PS/Z	NS/	ZO/	S/N	M/P	O/Z
PB	S	O	ZO	NM	M	M	O
	PM/	PM/	NB/	NB/	NS/P	PM/	NB/P
	NM/	NM/	NB/	NS/	S/N	NM/	B/PS
	NS	NB	NS	NB	M	NB	

IV. ANALYSIS OF SIMULATION RESULTS OF CHARGER

Figure 18 shows the simulation model of fuzzy PID control system based on the optimized fuzzy rules and membership function.

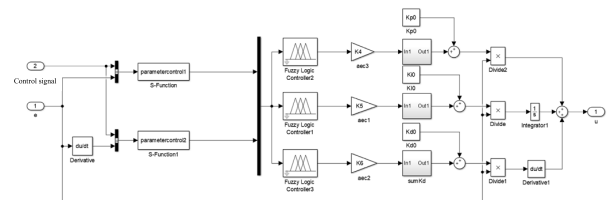


FIGURE 18. Simulation model of fuzzy-PID control system.

A. COMPARISON OF OUTPUT RESULTS OF DIFFERENT CONTROL METHODS AFTER SETTING EXPECTED VALUE

In this paper, a fuzzy PID control system is designed to compare the output data, and genetic algorithm is used to optimize the fuzzy PID to improve the control accuracy. The expected output current is 24A, and the simulation output effects of different control methods are observed.

Figure 19 shows the comparison of the current output data of the charger of the Qingyuan maglev train under the three control methods. It can be seen from Table 5 that the output performance of the charger under the fuzzy PID control optimized by genetic algorithm is better, the adjustment time is reduced to less than 0.1s, and the output fluctuation is reduced to $\pm 1.5\%$.

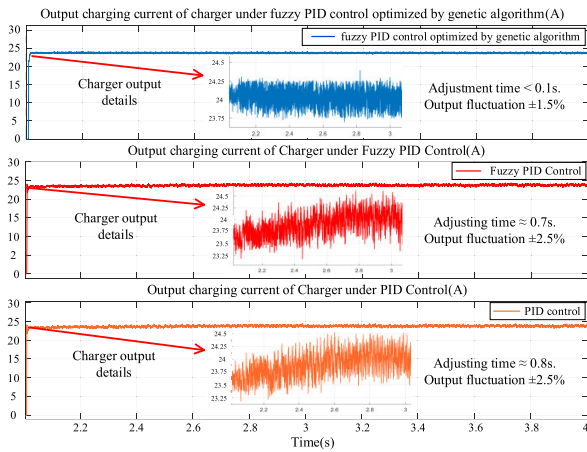


FIGURE 19. Optimization process of genetic algorithm.

TABLE 5. Performance comparison of different control methods under normal working conditions.

Control method	Performance	
	Adjustment time /s	Output fluctuation /%
PID	≈0.8	±2.5
Fuzzy PID	≈0.7	±2.5
Genetic algorithm optimized fuzzy PID	<0.1	±1.5

B. COMPARISON OF CHARGER RESULTS WHEN SWITCHING EXPECTED OUTPUT

The charger is set to change the expected output current at 5s, and the output characteristics of the charger under different control methods are shown in figure 20.

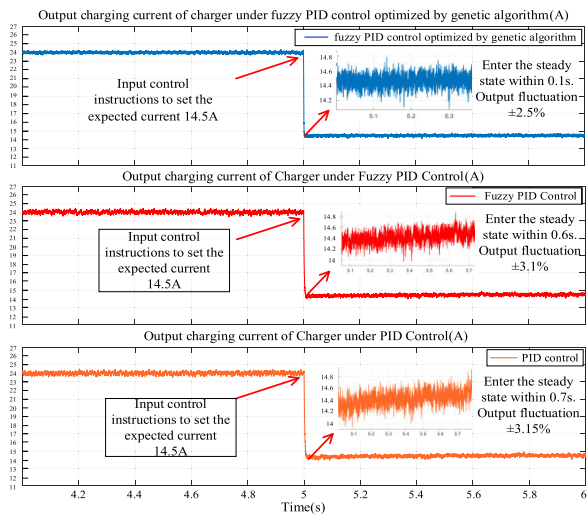


FIGURE 20. System simulation output with set current changed.

As can be seen from Table 6, the output performance of the optimized fuzzy PID control system is the best, and the optimized fuzzy charging control system needs less adjustment time to achieve the expected output within 0.1s, the overshoot is low, and the final output fluctuation is less than 2.5%.

TABLE 6. Performance comparison of different control methods under the condition of changing set current.

Control method	Performance	
	Adjustment time /s	Output fluctuation /%
PID	≈0.7	±3.15
Fuzzy PID	≈0.6	±3.1
Genetic algorithm optimized fuzzy PID	<0.1	±2.5

C. COMPARISON OF CHARGER RESULTS IN CASE OF DISTURBANCE

Set the expected charging current of the charger to 24A, add a disturbance signal with an amplitude of 10 and a duration of 0.01s at 7s, and observe the output result, as shown in figure 21 below.

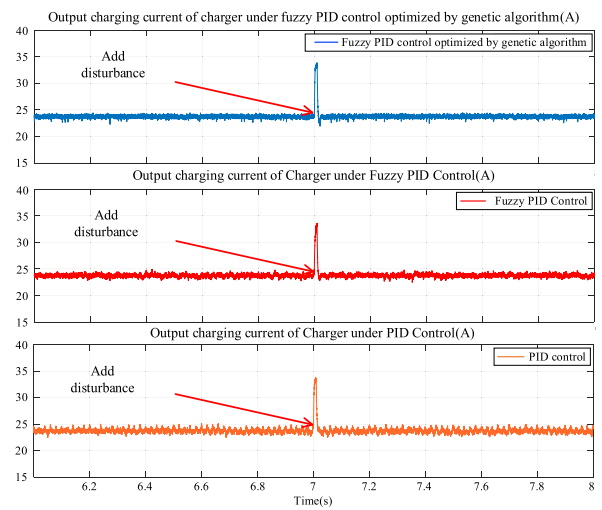


FIGURE 21. Simulation output of charger under disturbance.

From the simulation results, it can be seen that the charging control systems controlled by different methods under the influence of disturbance can restore stability in a fast time.

V. CONCLUSION

The main research object of the paper is the charger control system of Qingyuan maglev train. The charger control method is studied theoretically, and the charger simulation model is built. Through the analysis of the simulation results, a fuzzy PID charging control system optimized by genetic algorithm is designed on the basis of the original control system. The specific contents of this paper include:

- (1) The simulation model of Qingyuan maglev train charger is built in this paper. On the basis of meeting the requirements of the output results, the simulation output curve is compared with the output results of Qingyuan maglev train experimental platform, and the change trend of them is the same. The control research can be carried out in the simulation model.
- (2)The conventional PID control parameters cannot be adjusted adaptively, therefore, a fuzzy PID control method

is proposed based on fuzzy control theory. In view of the difficulty in determining the parameters of fuzzy PID membership function and the mismatch between fuzzy control rules and charger, a genetic algorithm program is designed to optimize the membership function and control rules of fuzzy PID.

(3) The fuzzy PID simulation model is built, and compared with the output results of the charger under different charging control methods, it is concluded that the fuzzy control system optimized by genetic algorithm can better reduce the error of the charger and improve the output response performance of the charger, which is of research significance.

REFERENCES

- [1] M.-A. Ocklenburg, M. Dohmen, X.-Q. Wu, and M. Helsen, "Next generation DC-DC converters for auxiliary power supplies with SiC MOSFETs," in *Proc. IEEE Int. Conf. Electr. Syst. Aircr., Railway, Ship Propuls. Road Vehicles Int. Transp. Electrific. Conf. (ESARS-ITEC)*, Nov. 2018, pp. 1–6.
- [2] I.-S. Lee, J.-Y. Kang, J. Lee, and S.-T. Lee, "Design considerations of auxiliary power supply unit with SiC MOSFET for lightweight railway vehicles," in *Proc. 21st Int. Conf. Electr. Mach. Syst. (ICEMS)*, Oct. 2018, pp. 908–915.
- [3] W. Jiang, "The HIL simulation modeling for EMU main and auxiliary integrated converter system," in *Proc. 7th IEEE Int. Symp. Microw., Antenna, Propag., EMC Technol. (MAPE)*, Oct. 2017, pp. 447–453.
- [4] D. Pefitsis, M. Antivachis, and J. Biela, "Auxiliary power supply for medium-voltage modular multilevel converters," in *Proc. 17th Eur. Conf. Power Electron. Appl. (EPE ECCE-Eur.)*, Sep. 2015, pp. 1–11.
- [5] D. Kan, S. Lina, D. Zhuohui, L. Yonghuan, and W. Nana, "Simulation study on temperature rising for the traction converter of high-speed EMUs," in *Proc. IEEE Power Eng. Autom. Conf.*, Sep. 2011, pp. 390–393.
- [6] Y.-H. Liu and Y.-F. Luo, "Search for an optimal rapid-charging pattern for Li-ion batteries using the Taguchi approach," *IEEE Trans. Ind. Electron.*, vol. 57, no. 12, pp. 3963–3971, Dec. 2010.
- [7] J.-M. Jo, Y.-J. Han, C. Y. Lee, J.-H. Lee, and H.-S. Jeong, "Analysis on the half bridge resonant DC to DC converter for electrical multiple units train set," in *Proc. 13th Int. Conf. Control, Autom. Syst. (ICCAS)*, Oct. 2013, pp. 424–426.
- [8] Y. Wang, W. Liu, T. Wang, X. Liu, Z. Chen, and Z. Yang, "Research on the modularization of the auxiliary power supply system of the high-speed train," in *Proc. Int. Conf. Elect. Inf. Technol. Rail Transp.* in Lecture Notes in Electrical Engineering, vol. 377, L. Jia, Z. Liu, Y. Qin, R. Ding, L. Diao, Eds. Berlin, Germany: Springer, 2016, pp. 461–472.
- [9] L. Zhang, L. Yun, M. Sun, and B. Peng, "Simulation research on auxiliary power supply system of China standard EMU," *Electronics*, vol. 8, no. 6, p. 647, Jun. 2019.
- [10] O. Akbatı, H. D. Üzgün, and S. Akkaya, "Hardware-in-the-loop simulation and implementation of a fuzzy logic controller with FPGA: Case study of a magnetic levitation system," *Trans. Inst. Meas. Control*, vol. 41, no. 8, pp. 2150–2159, May 2019.
- [11] K. Nithilasaravanan, N. Thakwani, P. Mishra, V. Kumar, and K. P. S. Rana, "Efficient control of integrated power system using self-tuned fractional-order fuzzy PID controller," *Neural Comput. Appl.*, vol. 31, no. 8, pp. 4137–4155, Aug. 2019.
- [12] I. Seedadan and R. Wongsathan, "Fuzzy controller based maximum power point tracking technique of standalone photovoltaic module for lead-acid battery charging," in *Proc. 3rd Int. Conf. Control, Autom. Robot. (ICCAR)*, Apr. 2017, pp. 1–6.
- [13] S. Nag and K. Y. Lee, "Optimized fuzzy logic controller for responsive charging of electric vehicles," *IFAC-PapersOnLine*, vol. 52, no. 4, pp. 147–152, 2019.
- [14] D. J. Auxillia, "Parallel tuning of fuzzy tracking controller for deep submergence rescue vehicle using genetic algorithm," *Indian J. Marine Sci.*, vol. 46, no. 11, pp. 2228–2240, 2017.
- [15] R.-J. Wai, J.-D. Lee, and K.-L. Chuang, "Real-time PID control strategy for maglev transportation system via particle swarm optimization," *IEEE Trans. Ind. Electron.*, vol. 58, no. 2, pp. 629–646, Feb. 2011.
- [16] Y. Sun, J. Xu, G. Lin, W. Ji, and L. Wang, "RBF neural network-based supervisor control for maglev vehicles on an elastic track with network time delay," *IEEE Trans. Ind. Informat.*, vol. 18, no. 1, pp. 509–519, Jan. 2022, doi: 10.1109/TII.2020.3032235.
- [17] Y. Sun, J. Xu, H. Wu, G. Lin, and S. Mumtaz, "Deep learning based semi-supervised control for vertical security of maglev vehicle with guaranteed bounded airgap," *IEEE Trans. Intell. Transp. Syst.*, vol. 22, no. 7, pp. 4431–4442, Jul. 2021, doi: 10.1109/TITS.2020.3045319.



LI ZHANG was born in 1984. She received the master's degree from the Hebei University of Technology. She worked as a Senior Engineer at CRRC Tangshan Company, Ltd. Her main research interest includes the electrical design of rail transit vehicle.



LIWEI ZHANG was born in Hebei, China, in 1977. He received the B.S. and M.S. degrees in electrical engineering from Beijing Jiaotong University, China, in 1999 and 2002, respectively, and the Ph.D. degree from the Institute of Electrical Engineering, Chinese Academy of Sciences, China, in 2006. Since January 2006, he was working with Beijing Jiaotong University as a Professor. Currently, he is studying at the Politecnico di Torino as a Visiting Scholar for one year. His current research interests include wireless charging technology, power electronics, and motor control.



JIAWEI YANG was born in Hebei, in 1998. He received the master's degree in electrical engineering from Qinghai University, in 2016. He is currently pursuing the master's degree with the School of Electrical Engineering, Beijing Jiaotong University.



MING GAO was born in 1982. He received the bachelor's degree from the Hebei University of Science and Technology. He worked as an Engineer at CRRC Tangshan Company, Ltd. His main research interest includes the electrical design of rail transit vehicles.



YINGHUA LI was born in 1983. He received the master's degree from North China Electric Power University. He worked as a Senior Engineer at CRRC Tangshan Company, Ltd. His main research interest includes the electrical design of rail transit vehicles.

...